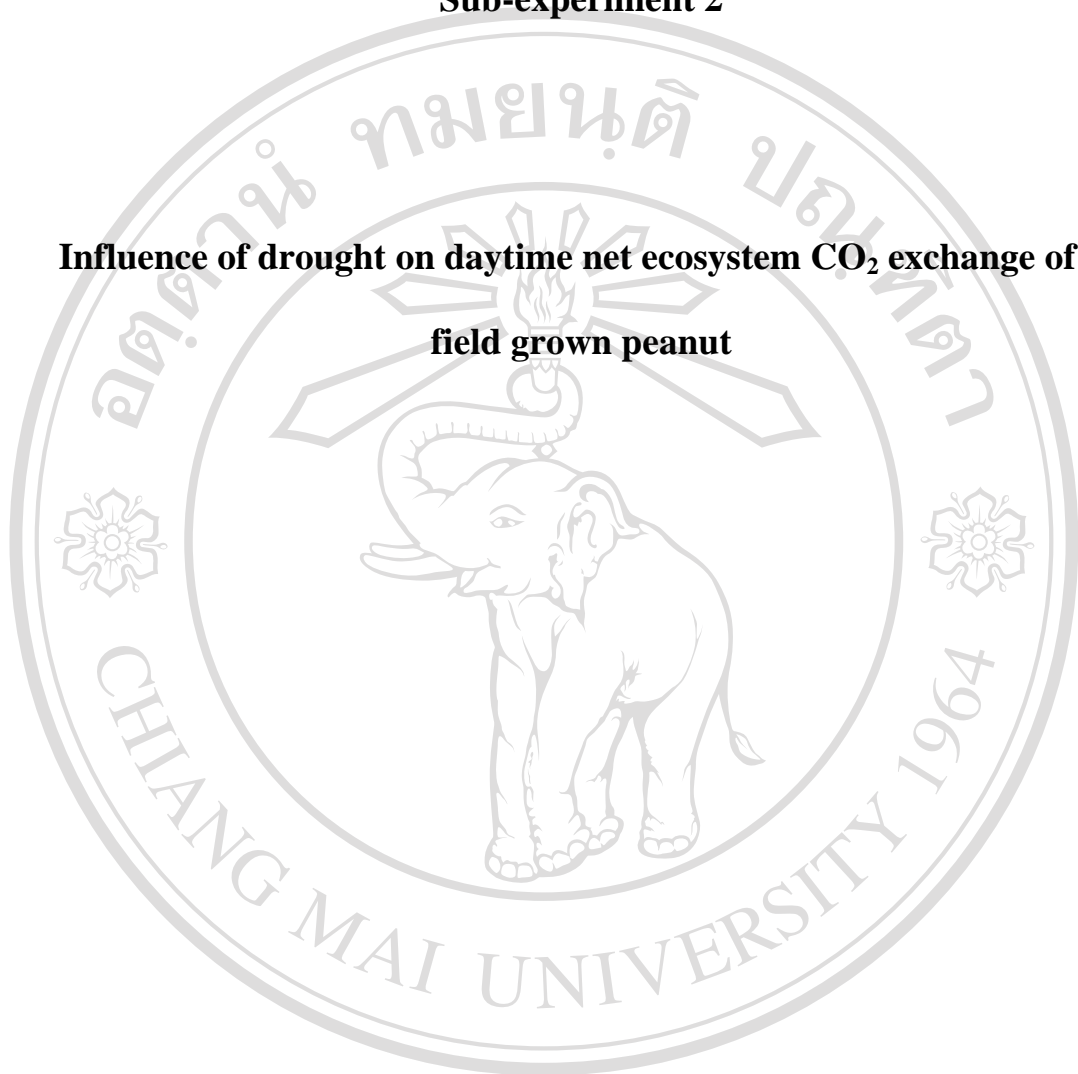


Sub-experiment 2

**Influence of drought on daytime net ecosystem CO₂ exchange of a
field grown peanut**



ลิขสิทธิ์มหาวิทยาลัยเชียงใหม่

Copyright© by Chiang Mai University

All rights reserved

INTRODUCTION

Concerns over global climate change have generated an effort to understand how environmental changes, such as those seen in temperature and precipitation, influence net carbon exchange between ecosystem and the atmosphere. The increased temperature and lower precipitation predicted in many regions of the world, is expected to adversely affect crop growth and water availability, critically influencing the patterns of future agricultural production. In light of these likely changes in regional precipitation and resulting soil moisture amounts, and because of the crucial role soil moisture plays in the carbon exchange. An understanding of how climate variability, particularly reductions precipitation, influences carbon exchange in the present ecosystem is a sine qua non condition to anticipate possible impacts of the climate change scenarios. This also provides the modeling community with a better basis to improve and validate their models.

Net ecosystem CO₂ exchange (*NEE*) relies on the balance between CO₂ uptake through plant photosynthesis and CO₂ emission through plant and soil respiration which refers to ecosystem respiration. The *NEE* can be measured directly using eddy-covariance methods (EC) (Aubinet *et al.*, 2000; Baldocchi *et al.*, 2001), which allows to measure spatially integrated carbon exchange on a continuous basis with minimal disturbance to the crop. With these continuous measurements the derivation of annual sums of net ecosystem CO₂ exchange or the integration over a vegetation period became possible. However, due to a combination of the limitations on the applicability of the measurement techniques and the robustness of the measurements

such as instrument failure or weather conditions, data rejection and missing data are unavoidable leading to 65-75% data coverage across the seasons (Baldocchi *et al.*, 2001; Falge *et al.*, 2001a; Law *et al.*, 2002). The resultant gaps in the time series must be reconstructed in order to obtain the seasonal carbon balance. Particularly, gap-filling techniques are based on a wide range of standard procedures, including linear interpolation (Falge *et al.*, 2001a), look-up table (Falge *et al.*, 2001a), moving averages (Falge *et al.*, 2001a; Reichstein *et al.*, 2005), non-linear regression (Falge *et al.*, 2001a; Goulden, 1996; Suyker and Verma, 2001), artificial neural networks (Papale and Valentini, 2003; Papale *et al.*, 2006), and multiple imputation method (Hui *et al.*, 2004).

By far however, the traditional standard method to gap *NEE* data during the daytime has been the non-linear regression. This approach is based on parameterized non-linear equations to quantify the relationship between *NEE* and light. While the failure using non-linear equation to describe daytime *NEE* only as a function of light has been previously observed in various ecosystem (Holst *et al.*, 2008; Li *et al.*, 2005; Serrano-Ortiz *et al.*, 2007; Wang *et al.*, 2008), to date a mechanistic explanation of this failure is still missing. To this end, the EC method was conducted in a rainfed peanut field during growing season. The objective of the present study are to examine the influence of drought stress on daytime *NEE* and to explain the inability of using the Michaelis-Menten equation to describe *NEE-PAR* relationship.

MATERIALS AND METHODS

Site description, experimental measurements and data processing were described in the sub-experiment 1.

Data Analysis

During daytime, defined as period with solar radiation $> 20 \text{ W m}^{-2}$, half-hourly data were fitted using a the Michaelis-Menten equation (Michaelis and Menten, 1913) to test the ability of the following model to describe the anticipated dependence of NEE ($\mu\text{mol CO}_2 \text{ m}^{-2} \text{ s}^{-1}$) on solar PAR ($\mu\text{mol photons m}^{-2} \text{ s}^{-1}$):

$$NEE = \frac{\alpha \cdot PAR \cdot NEE_{sat}}{\alpha \cdot PAR + NEE_{sat}} + R_e, \quad (3.1)$$

where α is the apparent quantum yield or the initial slope of the light response curve ($\mu\text{mol CO}_2 \mu\text{mol}^{-1} \text{ photons}$), NEE_{sat} is the saturation value of NEE at an infinite light level, and R_e is the ecosystem respiration during the daytime. Incident photosynthetically active radiation (PAR) was estimated from solar radiation: PAR ($\mu\text{mol photons m}^{-2} \text{ s}^{-1}$) = $2.16 \times \text{solar radiation (W m}^{-2}\text{)}$ (Weiss and Norman, 1985).

RESULTS AND DISCUSSION

Responses of daytime *NEE* to *PAR*

PAR is the main climatic factor that drives photosynthesis processes. To examine how *NEE* responds to change in *PAR*, a rectangular hyperbolic Michaelis-Menten function (Equation 3.1) was used to describe these responses in the 30-min resolution (Figure 3.1). In general, the peanut is a fast-growing crop and therefore the functional response of *NEE* to *PAR* was considered with respect to the growing stage (Table 3.1). During the study period, the rectangular hyperbolic function can be used to describe the relationship between *NEE* and *PAR* with success. Other than during DOY 219-226 and DOY 227-234, which their temperature (32 ± 4.1 and 31.5 ± 4.1 °C, respectively) and *VPD* (20.0 ± 11.8 and 20.6 ± 11.9 hPa, respectively) were high and *SWC* (0.037 ± 0.002 and 0.048 ± 0.020 m³ m⁻³, respectively) was very low (Table 1), the Michaelis-Menten function failed to describe *NEE-PAR* relationship. It is worth nothing the large scatter of the data points at these periods (Figure 3.1c), which apparently illustrates the dependence of *NEE-PAR* relationship on other environmental factors, as discuss later. Based on the statistical analysis using Equation 3.1, the regression coefficients indicated that change in *PAR* accounted for 67 to 89 % of the variations in *NEE*. The α values varied from -0.0183 to -0.0438 $\mu\text{mol CO}_2 \mu\text{mol}^{-1}$ photons. This value was well within the range of α reported for crops and grasslands (-0.008 to -0.465 $\mu\text{mol CO}_2 \mu\text{mol}^{-1}$ photons; Ruimy *et al.*, (1995); Suyker *et al.* (2004); Suyker and Verma (2001); Valentini *et al.*, (1995)). The

low α at the end of study period was most likely due to peanut was in the senescent phase.

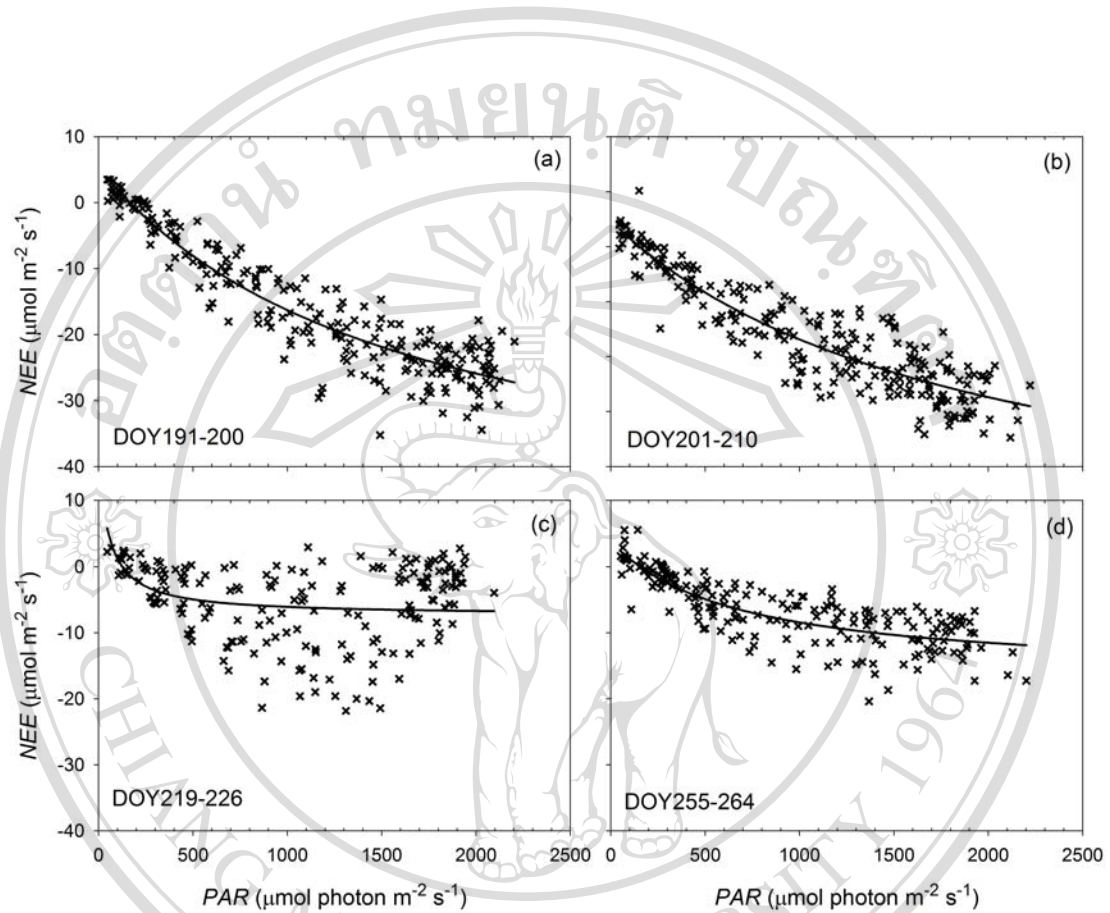


Figure 3.1 Example of light response curves at different growth stages during the study period. The Michaelis-Menten equation as described in Equation 3.1 was used to fit the data, and the regression coefficients are presented in Table 3.1.

Table 3.1 Values of the parameters describing features of the Michaelis-Menten function responses of daytime net ecosystem CO₂ exchange (*NEE*) to incident photosynthetically active radiation (*PAR*) (Equation 3.1)

Treatment	LAI (m ² m ⁻²)	SWC (m ³ m ⁻³)	T _a (°C)	VPD (hPa)	α (μmol μmol ⁻¹)	NEE _{sat} (μmol CO ₂ m ⁻² s ⁻¹)	R _e (μmol CO ₂ m ⁻² s ⁻¹)	n	R ²
DOY 181-190	4.72	0.073 ± 0.026	27.1 ± 3.3	12.2 ± 7.1	-0.0358 ± 0.0061	-35.69 ± 2.08	5.35 ± 1.06	235	0.78
DOY 191-200	4.55	0.061 ± 0.018	27.9 ± 3.1	12.0 ± 7.0	-0.0350 ± 0.0041	-56.22 ± 3.76	5.27 ± 0.96	234	0.88
DOY 201-210	6.00	0.074 ± 0.035	27.3 ± 3.4	12.3 ± 6.9	-0.0328 ± 0.0044	-62.58 ± 6.26	4.65 ± 1.06	244	0.84
DOY 211-218	7.81	0.065 ± 0.029	28.8 ± 3.3	12.8 ± 7.3	-0.0359 ± 0.0069	-51.35 ± 4.87	6.14 ± 1.54	192	0.76
DOY 219-226		0.037 ± 0.002	32.1 ± 4.1	20.0 ± 11.8	-0.4306 ± 0.9883*	-24.02 ± 21.67*	16.68 ± 22.17*	188	0.10
DOY 227-234	2.92	0.048 ± 0.020	31.5 ± 4.1	20.6 ± 11.9	-0.0921 ± 0.1226*	-18.71 ± 6.92	8.60 ± 7.96*	183	0.16
DOY 235-244	5.06	0.088 ± 0.025	26.8 ± 3.0	7.0 ± 5.2	-0.0321 ± 0.0036	-50.23 ± 3.70	5.22 ± 0.78	194	0.89
DOY 245-254	4.74	0.050 ± 0.023	27.6 ± 2.9	13.1 ± 7.0	-0.0438 ± 0.0091	-28.72 ± 1.18	5.63 ± 1.26	233	0.75
DOY 255-264		0.064 ± 0.024	24.4 ± 3.1	8.0 ± 5.0	-0.0305 ± 0.0077	-20.56 ± 1.17	3.87 ± 1.04	203	0.67
DOY 265-271	4.06	0.075 ± 0.016	26.3 ± 3.3	8.9 ± 6.4	-0.0183 ± 0.0057	-19.06 ± 2.19	4.03 ± 1.00	129	0.69

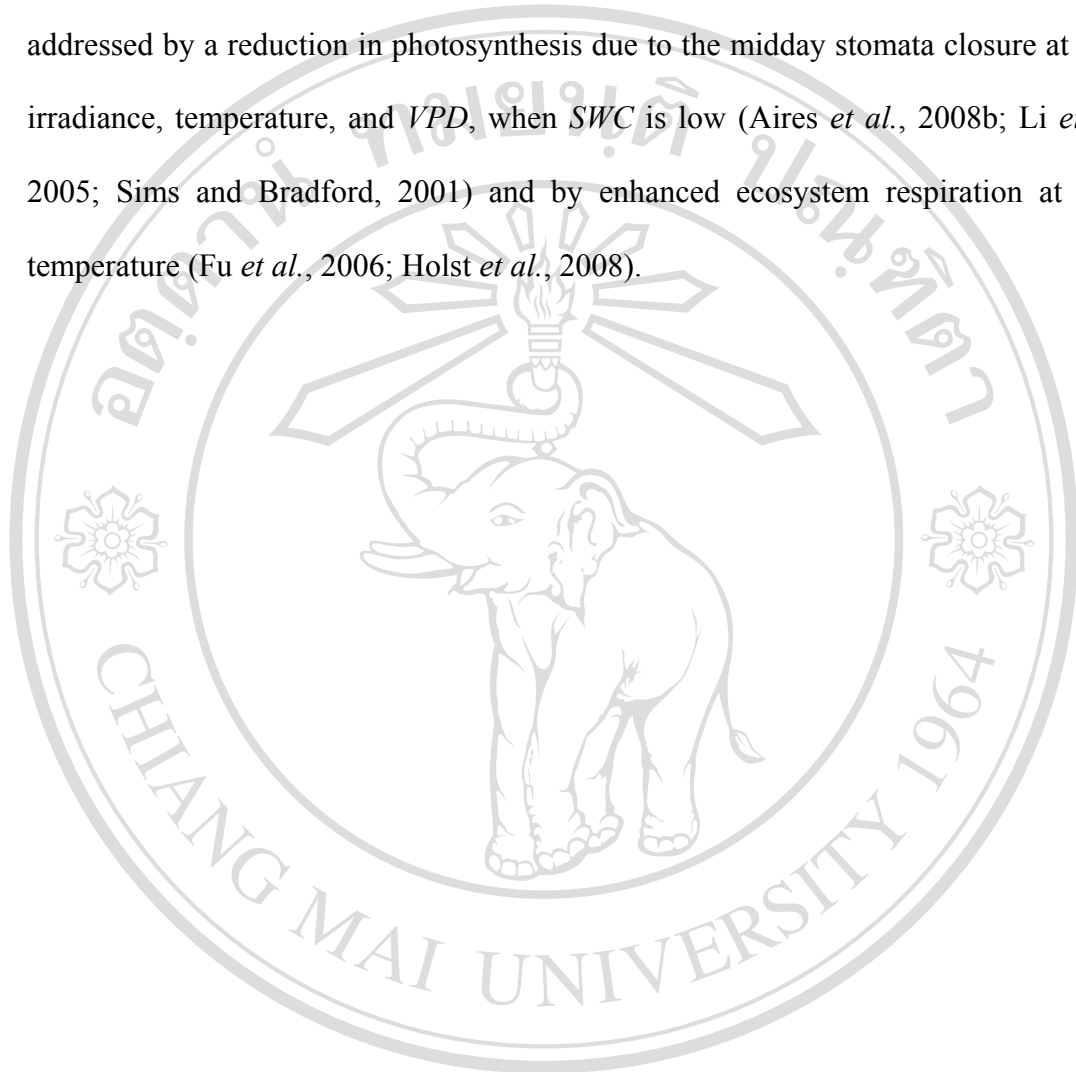
* not significant at $P \leq 0.05$; LAI, leaf area index; SWC, soil water content at 2-5 cm depth; T_a, air temperature at 2 m above the ground; VPD, atmospheric water vapor deficit at T_a; α, the apparent quantum yield; NEE_{sat}, the saturation value of NEE at an infinite light level not significant; R_e, the ecosystem respiration during daytime; n, observation; and R², the coefficient of determination

In order to further examine the dependence of *NEE-PAR* response on T_a , *VPD*, and *SWC*, daytime *NEE* obtained during the peak growing stage (DOY 201-240) were separate into three T_a classes ($T_a < 28$ °C, $28 < T_a < 32$ °C, and $T_a > 32$ °C), three *VPD* classes ($VPD < 10$ hPa, $10 < VPD < 20$ hPa, and $VPD > 20$ hPa), and three *SWC* classes ($SWC < 0.04$ m³ m⁻³, $0.04 < SWC < 0.07$ m³ m⁻³, and $SWC > 0.07$ m³ m⁻³) (Figure 3.2a, b, and c). Within each group, the *NEE* data were further subdivided by *PAR* into 200 $\mu\text{mol photons m}^{-2} \text{s}^{-1}$ increments ranging from 0 to 2200 $\mu\text{mol CO}_2 \mu\text{mol}^{-1}$ photons and then were bin averaged for each *PAR* subgroup.

Irrespective of T_a , *NEE* increased with *PAR* increased at all temperature conditions (Figure 3.2a). These results are in general agreement with previous findings demonstrating that peanuts perform well in the temperature range between 24 to 33 °C (Saxena *et al.*, 1983). However, at high temperature range ($T_a > 32$ °C), *NEE* was lower than the other two temperature ranges. Similar to T_a , *NEE* increased with *PAR* increased at all *VPD* ranges (Figure 3.2b). *NEE-PAR* response curves at $VPD < 10$ hPa and $10 < VPD < 20$ hPa mostly overlapped each other, indicating that there were no significant effects on *NEE-PAR* relationships between these two *VPD* ranges.

When peanut was subjected to high *VPD* (> 20 hPa), *NEE* was lower than the other two *VPD* conditions. Unlike T_a and *VPD*, there were pronounced differences in the light response curves among different soil water regimes (Figure 3.2c). When *SWC* was not limiting ($SWC > 0.04$ m³ m⁻³), *NEE* increased with *PAR* and there was no indication of canopy light saturation. For very low *SWC* (< 0.04 m³ m⁻³), *NEE* increased with *PAR* at first and get considerably decreased (*NEE* gets more positive resulted from ecosystem loss carbon to the atmosphere) when *PAR* exceeded 1300 $\mu\text{mol photons m}^{-2} \text{s}^{-1}$. A reduction in *NEE* in dry conditions has been observed for

different ecosystems (Aires *et al.*, 2008b; Fu *et al.*, 2006; Hastings *et al.*, 2005; Holst *et al.*, 2008; Li *et al.*, 2005; Sims and Bradford, 2001; Wang *et al.*, 2008) and could be addressed by a reduction in photosynthesis due to the midday stomata closure at high irradiance, temperature, and *VPD*, when *SWC* is low (Aires *et al.*, 2008b; Li *et al.*, 2005; Sims and Bradford, 2001) and by enhanced ecosystem respiration at high temperature (Fu *et al.*, 2006; Holst *et al.*, 2008).



ลิขสิทธิ์มหาวิทยาลัยเชียงใหม่
Copyright© by Chiang Mai University
All rights reserved

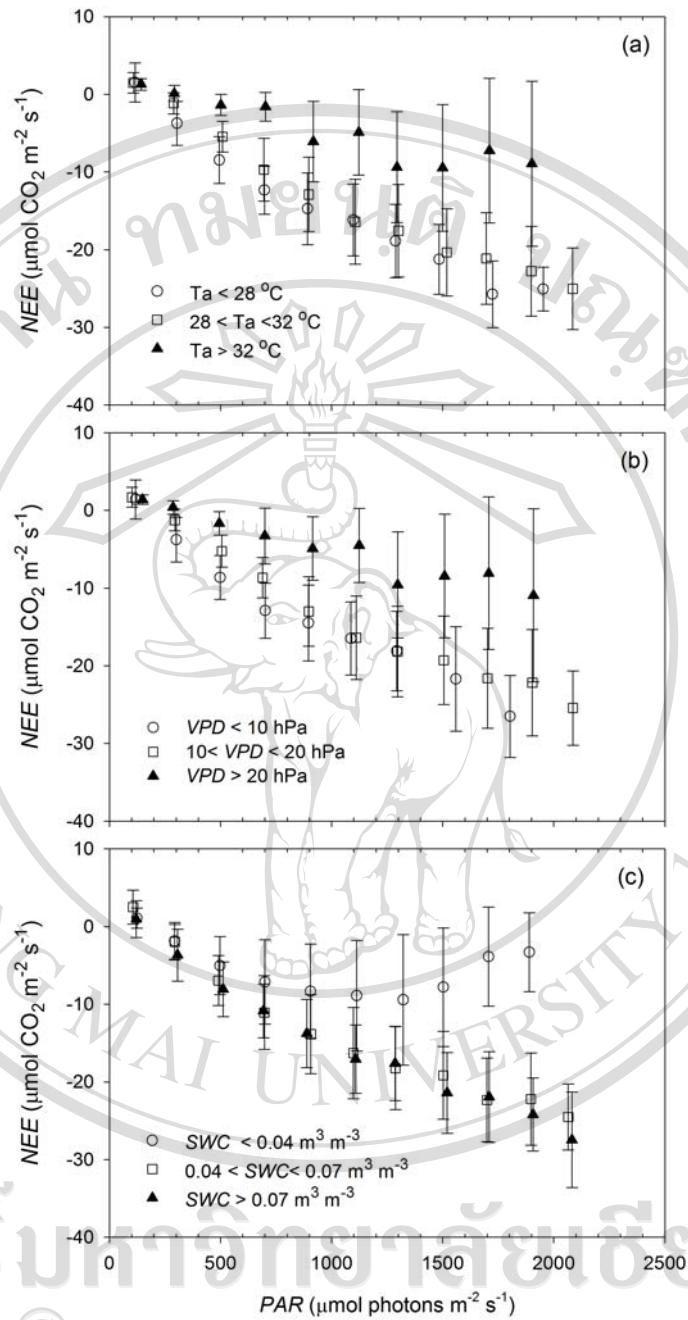


Figure 3.2 Relationship between net ecosystem CO_2 exchange (NEE) and photosynthetically active radiation (PAR) under (a) different air temperature (T_a), (b) different vapor pressure deficit (VPD), and (c) under different soil water content (SWC) during the peak growing stages (DOY 201-240). NEE data were averaged with PAR bins. Bin width is $200 \mu\text{mol photons m}^{-2} \text{s}^{-1}$. Bars indicate standard deviations.

Responses of daytime *NEE* to water stress

As discussed above, carbon uptake in this ecosystem is the result of several interaction factors, including *PAR*, *LAI*, T_a , *VPD*, and *SWC*. Among these factors, *SWC* was cited as the dominant factor limiting the *NEE-*PAR** response of peanut during the peak growing stages (Figure 3.2c). To illustrate the underlying physiological mechanisms of depression of *NEE*, the diurnal course of *NEE* and surface conductance (g_s) on clear days under two contrasting conditions were investigated. On the non-stress days with an average of daytime *SWC* of $0.075 \pm 0.026 \text{ m}^3 \text{ m}^{-3}$, similar variation trends were observed for T_a and *VPD*. T_a and *VPD* increased over the daytime reaching the maximum at $31.7 \pm 1.4 \text{ }^\circ\text{C}$ and $20.5 \pm 3.9 \text{ hPa}$, respectively, in the late afternoon (Figure 3.3a). *NEE* increased to a maximum of $26.71 \pm 5.72 \text{ } \mu\text{mol CO}_2 \text{ m}^{-2} \text{ s}^{-1}$ at about midday and then decreased as the afternoon progressed (Figure 3.3b). The maximum g_s appeared around noon, which indicates sufficient water available for the ecosystem (Figure 3.3b). On the water stress days with the average of *SWC* of $0.037 \pm 0.002 \text{ m}^3 \text{ m}^{-3}$, the diurnal course of T_a and *VPD* were similar to those on the non-stress days, but the maximum values ($36.9 \pm 1.6 \text{ }^\circ\text{C}$ for T_a , $39.3 \pm 8.3 \text{ hPa}$ for *VPD*) were much higher than the non-stress days (Figure 3.3c). The diurnal trends of *NEE* followed a pattern similar to g_s , which increased to a maximum ($15.98 \pm 3.16 \text{ } \mu\text{mol CO}_2 \text{ m}^{-2} \text{ s}^{-1}$ for *NEE*, $0.0107 \pm 0.0074 \text{ m s}^{-1}$ for g_s) around mid-morning and then rapidly declined throughout the remainder of the day as *VPD* increased (Figure 3.3d). The reduction of photosynthesis under dry conditions is usually caused by either stomatal or non-stomatal limitations. The former could be partially attributed to stomatal closure, while the latter could be the decrease of leaf photosynthetic activity which can lead to irreversible reduction of plant

photosynthesis (Bhagsari *et al.*, 1976; Fu *et al.*, 2006; Reddy *et al.*, 2003b). It is evident that the reduction of photosynthesis was related to the variation of g_s with water stress (Aires *et al.*, 2008b; Anthony *et al.*, 2002). Aires *et al.* (2008b) and Oguntunde (2005) indicated that VPD plays a strong role in controlling g_s when the soil moisture is not adequate. Figure 3.4 illustrates the dependence of g_s on VPD under water stress days. Without the limitation of PAR ($> 1000 \mu\text{mol photons m}^{-2} \text{s}^{-1}$), decreasing in g_s with increasing VPD was observed (Figure 3.4). It was found that 95% of variance in g_s was explained by the changes in VPD , indicating that g_s are sensitive to VPD in the present study.

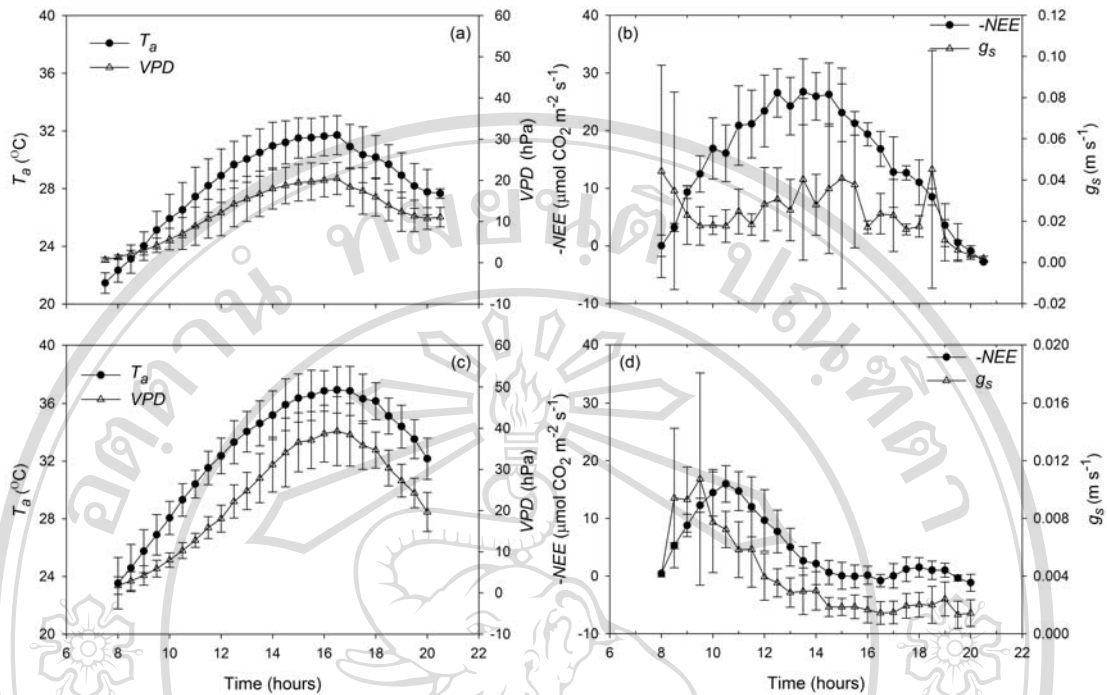


Figure 3.3 Diurnal variations of negative net ecosystem CO₂ exchange ($-NEE$), surface conductance (g_s) and correspondingly environmental factors of air temperature (T_a) and vapor pressure deficit (VPD) on clear days under non-stress condition (a and b, measured on DOY 210, 212, 213, 214, and 216) and water stress condition (c and d, measured on DOY 220, 222, 225, 226, and 227). Bars indicate standard deviations.

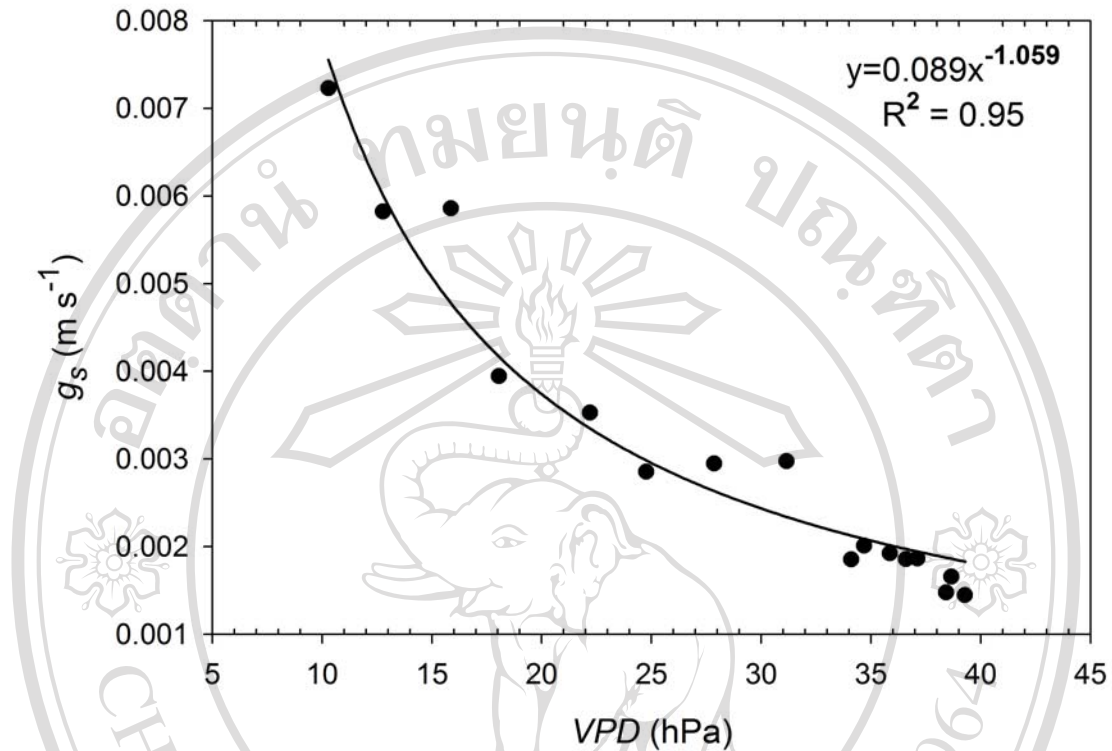


Figure 3.4 Response of half-hour surface conductance (g_s) to vapor pressure deficit (VPD) during water stress condition (measured on DOY 220, 222, 225, 226, and 227) when $PAR > 1000 \mu\text{mol photons m}^{-2} \text{s}^{-1}$.

The limitation of using non-linear regression to describe the *NEE- PAR* relationship has been well documented in the water-limited ecosystems (Holst *et al.*, 2008; Li *et al.*, 2005; Serrano-Ortiz *et al.*, 2007; Wang *et al.*, 2008). However, the mechanistic explanation of the processes inducing this limitation is still missing. The distinct hysteresis loop was evident in the relationship between *NEE* and *PAR* for both non-stress and water stress days (Figure 3.5a, b). However, the hysteresis loop was much reduced in area on the non-stress days as compared to the water stress days. On the non-stress days, as *PAR* increased in the morning, *NEE* increased (gets more negative) and as *PAR* decreased in the afternoon, *NEE* declined (Figure 3.5a). The result suggests that T_a , *VPD*, and *SWC* are not the limiting factors in the *NEE- PAR* response. Under water stress, as *PAR* increased in the morning, *NEE* increased, reaching the peak value at *PAR* of $1100 \mu\text{mol photons m}^{-2} \text{ s}^{-1}$ and then rapidly decreased, reaching almost zero at the end of morning. As *PAR* decreased, *NEE* remained constant nearly zero throughout the afternoon (Figure 3.5b). Hysteresis has been found in the responses of *NEE* to *PAR* in a tropical transitional forest in Brazilian Amazon (Vourlitis *et al.*, 2005). Counterintuitively, a magnitude of hysteresis was observed during the dry season than in the wet season (Vourlitis *et al.*, 2005). Causes of hysteresis in the response of *NEE* to *PAR* remain poorly understood.

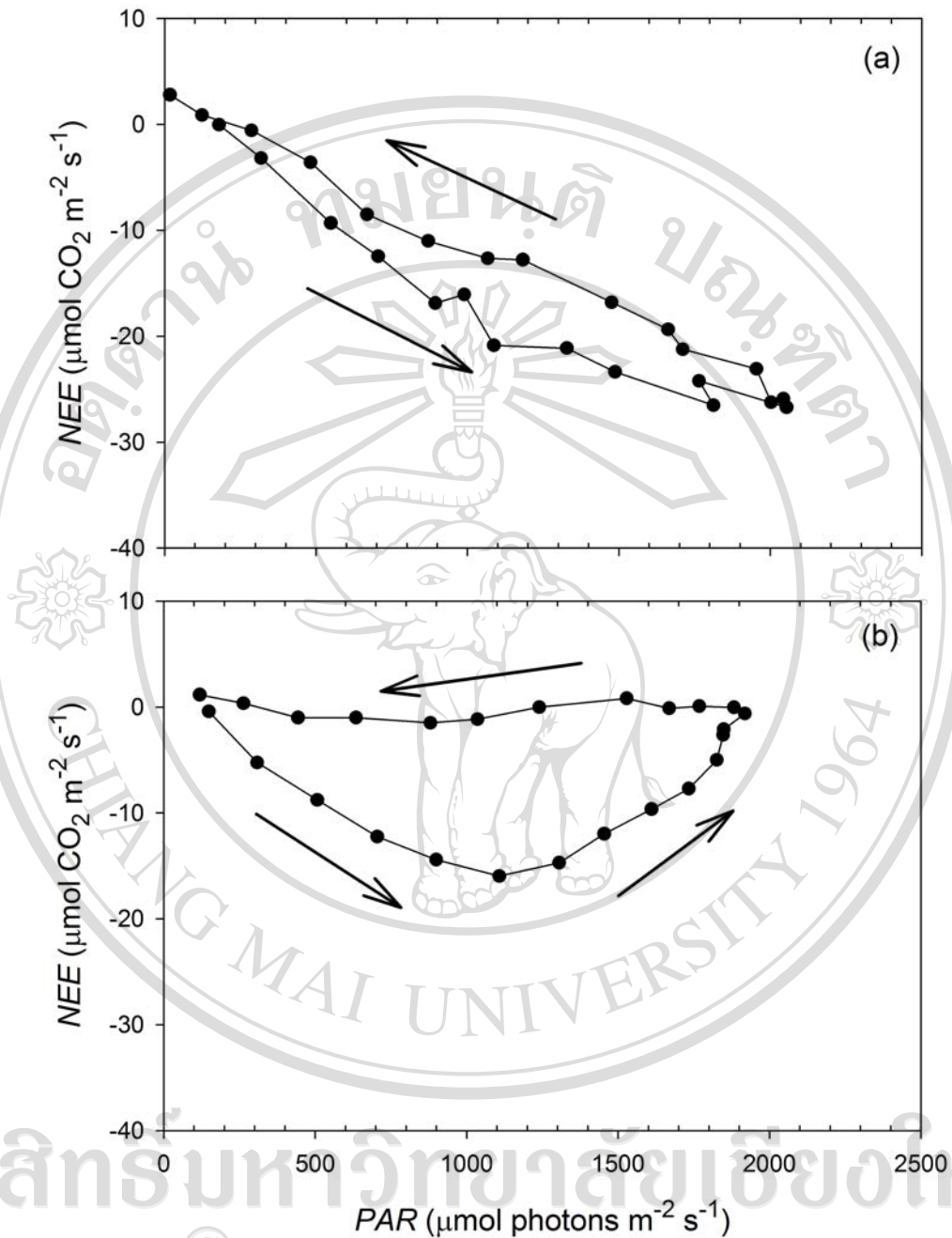


Figure 3.5 The relationship between photosynthetically active radiation (*PAR*) and net ecosystem CO₂ exchange (*NEE*) on clear days under (a) non-stress condition (measured on DOY 210, 212, 213, 214, and 216) and (b) water stress condition (measured on DOY 220, 222, 225, 226, and 227). The arrows indicate the direction of the hysteresis effect.

Hysteresis occurs when an increase in a given independent variable, x does not cause the same response in a dependent variable, y , when variable x decreases (Zeppel *et al.*, 2004). In the morning, as PAR increased, carbon uptake increased, but in the afternoon, carbon uptake at any given PAR was lower than the rate in the morning at the same PAR . A counter-clockwise rotation in the response curve was present, for both non-stress and water stress days (Figure 3.5a, b). The reason that the magnitude of hysteresis for the water stress days is larger than that for the non-stress days was related to the variation of g_s with water stress. The observed decrease in g_s with increasing VPD (Figure 3.4) corresponds to a decrease in carbon uptake on the water stress days, indicating strong stomatal control. Stomatal sensitivity to VPD increased in the afternoon and therefore the degree of closure increased, causing a reduce carbon uptake. The stomatal limitation caused by soil water insufficiency was responsible for a large of hysteresis loop. The consistent presence of hysteresis limited the ability of non-linear equation (Michaelis-Menten function) to adequately predict daytime NEE as a function of light.